

Ketene Formation or Phenyl-Group Migration as the Favorable Intramolecular Rearrangement in Phenyliodonium Ylides of Hydroxyquinones

Evangelos G. Bakalbassis,^[a] Spyros Spyroudis,^[b] and Constantinos A. Tsipis^[a]

Keywords: Density functional calculations / Transition states / Ylides / Quinones

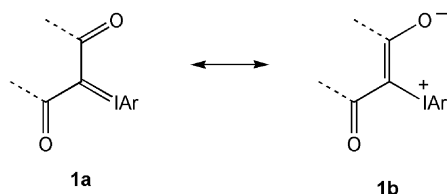
Phenyliodonium ylides of hydroxyquinones easily undergo intramolecular rearrangements associated with phenyl-group migration or ketene formation under ambient conditions. The mechanism of the two rival potential reaction paths was explored by electronic structure calculation techniques at the B3LYP/6-311+G(d,p)USDD(I) level. It was found that both rearrangements follow a single-step concerted mechanism occurring via a four-membered [1.1.0] bicyclic ring transition state for the ketene-formation process and a five-membered transition state for the phenyl-group migration process. The ketene-formation pathway is predicted to be kinetically and thermodynamically more favorable than the phenyl-group migration pathway, and this is in excellent agreement with the experimental findings that

these ylides predominantly form ketenes. An alternative pathway to ketene formation that involves intramolecular rearrangement through a singlet-carbene transition state resulting from dissociation of iodobenzene was also examined. This process was found to be kinetically unfavorable, as it demanded a relatively high activation barrier of 40.6 kcal mol⁻¹. The geometric and energy reaction profile of both intramolecular rearrangements were thoroughly scrutinized, whereas the electronic effects accompanying the intramolecular rearrangements were analyzed by means of electronic structure calculation methods.

(© Wiley-VCH Verlag GmbH & Co. KGaA, 69451 Weinheim, Germany, 2008)

Introduction

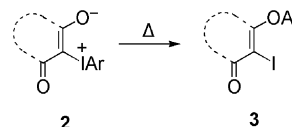
Zwitterionic iodonium compounds (ZIC) constitute an important class of hypervalent iodine compounds.^[1] Among ZIC, aryl-iodonium ylides of β -dicarbonyl compounds, represented in Scheme 1 in both their ylidic and zwitterionic structures, is perhaps the most well-studied group, as the diversity in their reactivity broadens their use as flexible building blocks in organic synthesis.^[2] This reac-



Scheme 1. Ylidic and zwitterionic resonance structures of aryl-iodonium ylides of β -dicarbonyl compounds.

tivity arises mainly from the fission of the I-C_{anionic} bond and depends mostly on the nature of the β -dicarbonyl moiety.

An interesting feature of the chemistry of the ylides of cyclic β -diketones is the thermal migration of the aryl group from the iodine atom to the oxygen atom, which always takes place at the *ipso* carbon atom of the aryl group bearing the I atom (Scheme 2). It is important to be noticed that such a migration was also observed in aryl-iodonium derivatives of phenolates.^[3]



Scheme 2. Aryl-group migration in aryl-iodonium ylides of cyclic 1,3-diketones.

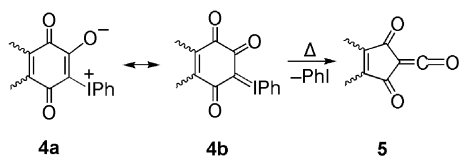
The mechanism of the aryl migration, first investigated by Nozaki et al.^[4] a long time ago, involves formation of a five-membered cyclic intermediate. In contrast, Moriarty^[5] very recently proposed a ligand coupling mechanism via four-membered cyclic intermediates. In a previous communication,^[6] by using electronic structure calculation techniques we proposed a concerted mechanism for the aryl group migration, which proceeded through a five-membered ring transition state without the involvement of any intermediate.

[a] Laboratory of Applied Quantum Chemistry, Department of Chemistry, Aristotle University of Thessaloniki, Thessaloniki 54124, Greece
Fax: +30-2310-997738
E-mail: bakalb@chem.auth.gr

[b] Laboratory of Organic Chemistry, Department of Chemistry, Aristotle University of Thessaloniki, Thessaloniki 54124, Greece

Supporting information for this article is available on the WWW under <http://www.eurjoc.org> or from the author.

It is well known that all phenyliodonium ylides of cyclic β -dicarbonyl compounds bearing at least one ketonic carbonyl group easily undergo aryl migration. There is, however, a notable exception: phenyliodonium ylides of 2-hydroxy-1,4-quinones **4** (Scheme 3) are exclusively transformed into α,α' -dioxoketenes **5** upon heating the suspensions of the ylides at reflux in dichloromethane or acetonitrile. No migration products analogous to **3** were detected in the reaction solution.



Scheme 3. Thermal transformation of phenyliodonium ylides of hydroxyquinones into α,α' -dioxoketenes.

The different behavior of the ylides with respect to their thermal transformation yielding quantitatively ketenes **5** triggered some interesting synthetic possibilities. Dioxoketenes analogous to **5** are very reactive and only a few have been reported in the literature.^[7] Ketenes **5** produced by thermal degradation of ylides **4** cannot be isolated, but they react further with water present in the solvent to afford, after subsequent decarboxylation of the intermediate acid, cyclopentene-1,3-diones, which can be used further as building blocks in synthesis.^[8] These ketenes can also be trapped by alcohols,^[8a] amines,^[9] and other amino compounds,^[10] as well as by carbon nucleophiles, such as indoles, pyrroles, and enamines^[11] to afford interesting enol structures. In addition, in the absence of nucleophiles, ketenes, namely, indenedione ketene, can dimerize in an unusual α -oxoketene [2+2] cycloaddition,^[11,12] and the quantitatively isolated oxetanone derivative exhibits an interesting and unusual type of reactivity.^[12] Considering the potential synthetic interest of the thermal ring contraction of phenyliodonium ylides of hydroxyquinones, we address herein, with the help of electronic structure calculation techniques, the mechanistic details and the understanding of their different reactivities in comparison to those of other analogous cyclic ylides.

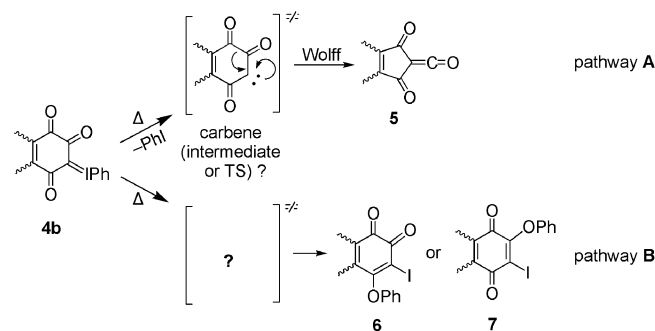
Computational Methodology

All stationary points (reactants, transition states, and products) located on the potential energy surfaces (PES) were fully optimized at the B3LYP/6-311+G(d,p) level of theory (the SDD^[13] basis set with relativistic effective core potentials was used for the I atom) as implemented in the Gaussian03 program suite.^[14] It should be stressed that the use of the above-mentioned large basis set for the heavy atoms and the H atoms was necessary in the present study, because a smaller one predicted a higher E_a value for the ketene-formation pathway than for the phenyl-group transformation pathway, which is not consistent with experimental results. All of the other ΔE_R values and the corresponding structural data of the reaction profiles, however, re-

mained unchanged in both basis sets used. The B3LYP method provides a good description of the reaction profiles, including geometries, heats of reactions, and barrier heights.^[15] Analytical frequencies were calculated at the same level of theory, and the nature of the stationary points was determined in each case according to the number of the negative eigenvalues of the Hessian matrix. ZPVE-scaled reaction energies, ΔE_R , are used for the discussion on both the relative stabilities of the chemical structures considered. For the determination of the geometries of the transition states, quasi-Newton transit-guided (QSTN) computations were performed.^[16] Moreover, the correct transition states were confirmed by intrinsic reaction coordinate (IRC) calculations, whereas intrinsic reaction paths (IRPs) were traced from the various transition structures to ensure that no additional intermediates existed.^[17] The wavefunctions of all stationary points were analyzed by natural bond orbital analyses, which included natural atomic orbital (NAO) populations and natural bond orbitals (NBO).^[18] Percent compositions of the molecular orbitals in terms of occupied and unoccupied fragment orbitals (FOs) of the appropriate molecular fragments interacting to form a particular bond, along with the respective orbital interaction diagrams, were calculated by the charge decomposition analysis (CDA) technique of Frenking and co-workers,^[19] as implemented in the AOMix program suite.^[20]

Results and Discussion

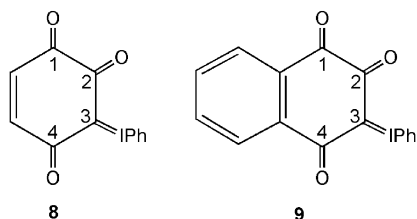
It was generally proposed (without real evidence) that the mechanism of the thermal degradation of ylides **4b** proceeds through carbene formation and subsequent Wolff rearrangement to ketenes **5** (Scheme 4, pathway A).^[8a–8c,9,10]



Scheme 4. Proposed mechanistic pathways for the intramolecular thermal rearrangements of phenyliodonium ylides of hydroxyquinones into α,α' -dioxoketenes through a carbene intermediate and/or transition state in the formation of ketene (pathway A) and in migration of the phenyl group (pathway B).

To verify whether carbenes are real intermediates or transition states and to explain why the migration reaction (Scheme 4, pathway B) does not take place at all, both reaction pathways were thoroughly explored. Phenyliodonium ylides of 2-hydroxy-1,4-benzoquinone **8** and 2-hydroxy-1,4-naphthoquinone **9**, for which experimental data are available, were selected as model compounds. The reaction steps involved in the entire thermal reaction course of **8** and **9**

have been scrutinized, and the transition states have been fully identified by monitoring the corresponding geometric and energetic reaction profile.



The geometric and potential energy reaction profiles for the migration of the phenyl group from the I atom to the O atom in **8** computed at the B3LYP/6-311+G(d,p)-USDD(I) level are depicted in Figure 1. The geometric and potential energy reaction profiles for phenyl-group migration in **9** are in complete analogy with those of **8** (see Supporting Information).

The energy data characterizing the phenyl-group migration processes of **8** and **9** are summarized in Table 1.

The phenyl group could migrate to the quinonic oxygen atoms in the 4- and/or 2-positions of the quinone ring to yield products **10** and **11**, respectively (Figure 1). The transformation of **8** into either **10** or **11** would proceed via transition states TS₈₋₁₀ and TS₈₋₁₁, surmounting activation barriers of 18.8 and 16.7 kcal mol⁻¹, respectively. These results illustrate that the thermal transformations of **8** into either **10** or **11** are of the same type and require gentle heating in solution. The normal coordinate vectors (arrows) of the vibrational modes, which correspond to the imaginary frequencies of TS₈₋₁₀ and TS₈₋₁₁ at 328*i* and 312*i* cm⁻¹, respec-

Table 1. Energy data (kcal mol⁻¹) for the phenyl-group migration processes in **8** and **9**.

	8	9
TS ₈₋₁₀ /TS ₉₋₁₀	18.8	18.4
TS ₈₋₁₁ /TS ₉₋₁₁	16.7	16.3
TS ₈₋₁₂ /TS ₉₋₁₂	11.6	11.4
Products 10 / 10' ^[a]	-35.2	-32.8
Products 11 / 11'	-39.5	-40.0
Products 12 / 12'	-48.5	-49.2

[a] Prime symbol corresponds to the products of ylide **9**.

tively, show that in both cases, the dominant motions involve the formation of a five-membered ring through weak C...I and C...O linkages; this transition-state ring structure resembles closely that of the analogous ylides of cyclic 1,3-diketones.^[6] The thermal phenyl-group migrations in **8** correspond to exothermic processes; the estimated ΔH_R values are 35.2 and 39.5 kcal mol⁻¹ for **10** and **11**, respectively. Perusal of Figure 1 reveals that the intramolecular phenyl-group migration in **8**, which yields product **11**, is both kinetically and thermodynamically more favorable than the phenyl-group migration in **8**, which yields product **10**, as a result of the lower activation energy and the higher exothermicity of the former transformation. The higher thermodynamic stability of **11** relative to that of **10** could be attributed to the *p*-quinoid structure of **11** in contrast to the *o*-quinoid structure of **10**. It is noteworthy that **9** showed a phenyl-group migration reaction profile that was quite analogous to that of **8**, and the corresponding energy data are close to each other. Moreover, the IRPs traced

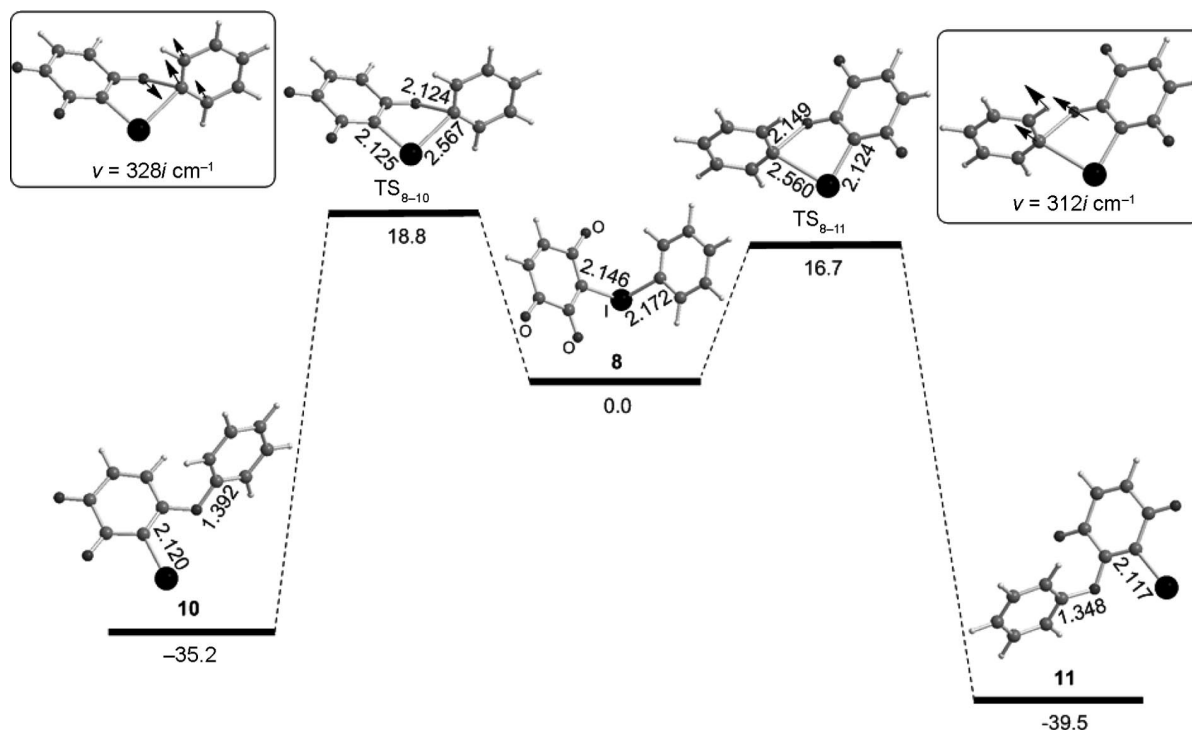


Figure 1. Geometric (bond lengths in Å) and potential energy (in kcal mol⁻¹) reaction profiles for phenyl-group migration from I to O in **8** computed at the B3LYP/6-311+G(d,p)USDD(I) level.

from the various transition structures verified that no further intermediates exist.

The easy migration of the phenyl-group in **8** could be understood on the basis of the ease with which the phenyl group undergoes dissociation owing to the relatively weak I–Ph interaction in **8**; the estimated interaction energy between the phenyl group and the iodoquinone fragment was found to be $-33.7 \text{ kcal mol}^{-1}$. Noteworthy is the electron spin-density distribution on the two fragments shown pictorially in Figure 2. The quinone O atom in the 2-position acquires higher spin density ($0.249 \text{ |e| bohr}^{-3}$) than the quinone O atom in the 4-position ($0.172 \text{ |e| bohr}^{-3}$). This is compatible with the higher probability for the phenyl group to migrate towards the O atom at the 2-position rather than at the 4-position.

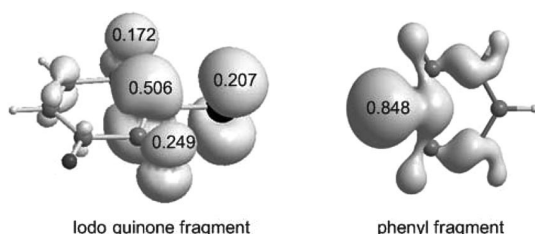


Figure 2. Representation of the spin-density map, along with the atomic spin densities, for iodoquinone and phenyl fragments computed at the B3LYP/6-311+G(d,p)USDD(I) level of theory. The isodensity surface represented corresponds to a value of $0.001 \text{ |e| bohr}^{-3}$.

Figure 3 shows the reaction profiles for the intramolecular formation of ketene in **8**. It is seen that the transformation of **8** into ketene **12** proceeds via transition state TS_{8-12} , surmounting an activation barrier of only $11.6 \text{ kcal mol}^{-1}$. The low activation barrier indicates that the thermal transformation $8 \rightarrow 12$ can easily occur even at

room temperature without any heating. This finding is in excellent agreement with the experimental finding that ketene, and not phenyl-group migration product **11**, is the exclusive product. The normal coordinate vectors (arrows) of the vibrational modes, which correspond to the imaginary frequency of TS_{8-12} at $282.8i \text{ cm}^{-1}$, illustrate that the dominant motions involve the formation of a very unusual, four-membered [1.1.0] bicyclic ring containing weak $\text{C}\cdots\text{I}$ and $\text{C}\cdots\text{O}$ linkages. Consequently, it is shown that the $8 \rightarrow 12$ intramolecular transformation is both kinetically and thermodynamically more favorable than the $8 \rightarrow 11$ phenyl-group migration as a result of the lower activation energy and the higher exothermicity of the former. It is noteworthy that **9** showed a ketene-formation reaction profile that was quite analogous to that of **8** (Table 1), which is also in excellent agreement with the corresponding experimental data.^[11,12] Moreover, the IRPs traced from the various transition structures ensured that no additional intermediates existed. Finally, attempts were made to explore the ketene-formation reaction profiles of the analogous ylides of cyclic 1,3-diketones, as well as the phenyl iodonium ylide of 2-amino-1,4-quinone, but all attempts failed at the DFT level. In contrast, we previously^[6] showed that in the latter case phenyl-group migration requires a lower energy of activation ($6.4 \text{ kcal mol}^{-1}$ from ref.^[6] and $7.9 \text{ kcal mol}^{-1}$ calculated at the present level of theory) than that required for the ketene-formation reactions in **8** or **9**.

The alternative pathway (Scheme 4, pathway A) for the intramolecular transformation $8 \rightarrow 12$, which proceeds through heterolytic C–I bond dissociation to yield a carbene and iodobenzene, was also explored. It was found that the carbene species, in its singlet state **13**, corresponds to a transition state with an imaginary frequency at $405i \text{ cm}^{-1}$. Carbene **13** can directly be transformed into the more stable ketene isomer **12**, or it could be stabilized in its triplet

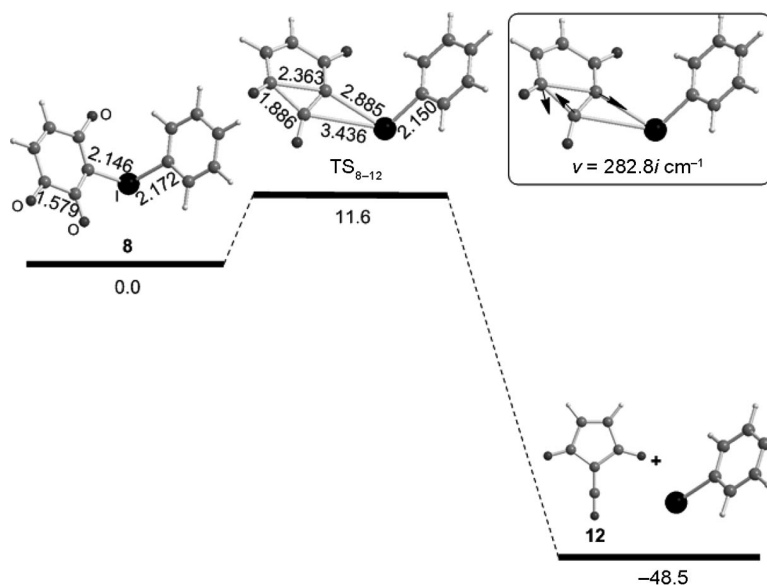


Figure 3. Geometric (bond lengths in Å) and potential energy (in kcal mol^{-1}) reaction profiles for the intramolecular formation of ketene in **8** computed at the B3LYP/6-311+G(d,p)USDD(I) level.

ground state (the stabilization energy amounts to $17.7 \text{ kcal mol}^{-1}$). Such a transformation corresponds to an exothermic process, and the estimated exothermicity was calculated to be $-48.5 \text{ kcal mol}^{-1}$ at the B3LYP/6-311+G(d,p)/USDD(I) level. However, the activation barrier for ketene formation via the carbene transition state (Scheme 4, pathway A) was predicted to be $46.0 \text{ kcal mol}^{-1}$, which is equal to the estimated interaction energy between the singlet-state carbene and the iodobenzene fragments. Hence, pathway A is not favored in the transformation $\mathbf{8} \rightarrow \mathbf{12}$ via singlet-state-carbene transition state $\mathbf{13}$.

The calculated natural net atomic charges on the quinone O(2) and O(4) atoms and the *ipso* aryl carbon atom of the 2,3,4-diketonic moiety in $\mathbf{8}$ are -0.62 , -0.58 , and $-0.47 |e|$, respectively ($\mathbf{9}$ shows analogous values). This negative-charge delocalization in both ylides, along with the high positive charges on the iodine atom ($+0.91 |e|$), could account for their stabilization. In addition, the negative natural net atomic charges on the *ipso* aryl carbon atom ($-0.20 |e|$) could exclude a charge-controlled mechanism for both the intramolecular phenyl-group migration and ketene-formation pathways. The orbital interaction diagram for the formation of the C_{ipso} -I bond is depicted schematically in Figure 4. This plot provides pictorial representation of the molecular orbital (MO) compositions and their contributions to chemical bonding.

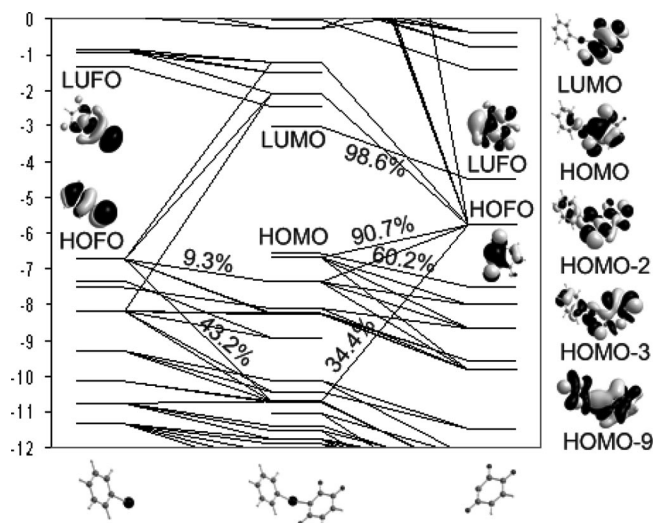


Figure 4. Orbital interaction diagram for the formation of the C_{ipso} -I bond in $\mathbf{8}$ on the basis of the interaction of the PhI and quinonic fragments computed at the B3LYP/6-311+G(d,p)/USDD(I) level.

Ylides $\mathbf{8}$ and $\mathbf{9}$ show analogous highest occupied (HOMO) and lowest unoccupied molecular orbitals (LUMO), mainly localized on the 1,3-diketonic moiety of their ring, and on the I and the *ipso* carbon atoms, respectively. The HOMO and LUMO of $\mathbf{8}$ resemble the highest occupied fragment orbital (HOFO) and lowest unoccupied fragment orbitals (LUFO) of the quinone fragment with compositions of 90.7 and 98.6%, respectively. The principal MOs contributing to C_{ipso} -I bond formation are HOMO-2, HOMO-3, and HOMO-9 and their compositions are

given in Figure 4. Thus, for example, HOMO-9 is a bonding orbital constructed from the overlap of the HOFOs of PhI and the quinonic fragments with compositions of 43.2 and 34.4%, respectively. The nature of the frontier orbitals of $\mathbf{8}$ suggests a frontier-orbital controlled mechanism for the intramolecular thermal transformations of the ylides under study. Moreover, the higher location of the HOMO on the quinone O atom in the 2-position than in the 4-position of $\mathbf{8}$ could account for the higher probability that *ipso* C attack occurs at the quinone O atom in the 2-position.

Conclusions

Electronic structure calculations at the B3LYP/6-311+G(d,p)/USDD(I) level illustrated that both ketene formation and phenyl-group migration in iodonium ylides, involving *p*-quinoid structures, follow analogous reaction pathways corresponding to a single-step, transition-state concerted mechanism. The transition state structures involve a very unusual, four-membered [1.1.0] bicyclic ring in the ketene-formation process and a five-membered ring in the phenyl-group migration process. Ketene formation is kinetically and thermodynamically more favorable than phenyl-group migration, which is in excellent agreement with the experimentally found exclusive formation of ketene in these ylides. In contrast, the suggested reaction pathway involving carbenes as intermediates or transition states is predicted to be kinetically unfavorable, as the estimated activation barrier is high ($40.6 \text{ kcal mol}^{-1}$) relative to the almost-negligible energy barrier for the concerted ketene-formation process. Finally, frontier-orbital-controlled mechanisms, supported by the respective intramolecular HOMO-LUMO interactions, seem probable in both cases.

Supporting Information (see footnote on the first page of this article): Cartesian coordinates and energies of all stationary points; phenyl-group migration and ketene-formation reaction profiles of ylide $\mathbf{9}$.

- [1] a) A. Varvoglis, *The Organic Chemistry of Polycordinated Iodine*, VCH, New York, **1992**, p. 307; b) G. F. Koser, *The Chemistry of Halides, Pseudo-Halides and Azides*, Wiley, New York, **1995**, p. 1173.
- [2] a) A. Varvoglis, *Hypervalent Iodine in Organic Synthesis*, Academic Press, London, **1997**; b) S. Spyroudis, A. Varvoglis, *Synlett* **1998**, 221–232; c) V. V. Zhdankin, P. Stang, *J. Chem. Rev.* **2002**, 102, 2523–2584; d) P. Müller, *Acc. Chem. Res.* **2004**, 37, 243–251.
- [3] a) P. B. Kokil, P. M. Nair, *Tetrahedron Lett.* **1977**, 18, 4113–4116; b) S. Spyroudis, A. Varvoglis, *J. Chem. Soc. Perkin Trans. 1* **1984**, 135–137; c) A. Georgantzi, S. Spyroudis, *Tetrahedron Lett.* **1995**, 36, 443–446; d) Y. R. Lee, Y. U. Yung, *J. Chem. Soc. Perkin Trans. 1* **2002**, 1309–1313.
- [4] M. Takaku, Y. Hayashi, H. Nozaki, *Tetrahedron* **1970**, 26, 1243–1247.
- [5] R. M. Moriarty, *J. Org. Chem.* **2005**, 70, 2893–2903.
- [6] E. G. Bakalbassis, S. Spyroudis, E. Tsiotra, *J. Org. Chem.* **2006**, 71, 7060–7062.
- [7] a) C. Wentrup, W. Heilmayer, G. Kollenz, *Synthesis* **1994**, 1219–1248; b) A. Stadler, K. Zangger, F. Belaj, G. Kollenz, *Tetrahedron* **2001**, 57, 6757–6763; c) B. C. Wallfisch, F. Belaj, C. Wentrup, C. O. Kappe, G. Kollenz, *J. Chem. Soc. Perkin*

- Trans. I* **2002**, 599–605; d) T. T. Tidwell, *Ketenes*, John Wiley & Sons, New Jersey, **2006**.
- [8] a) I. Papoutsis, S. Spyroudis, A. Varvoglis, *Tetrahedron Lett.* **1994**, 35, 8449–8452; b) S. Spyroudis, N. Xanthopoulou, *J. Org. Chem.* **2002**, 67, 4612–4614; c) S. Spyroudis, N. Xanthopoulou, *ARKIVOC* **2003**, vi, 95–105; d) G. Mehta, S. R. Singh, *Tetrahedron Lett.* **2005**, 46, 2079–2082; e) G. Mehta, S. R. Singh, *Angew. Chem. Int. Ed.* **2006**, 45, 953–955.
- [9] E. Malamidou-Xenikaki, S. Spyroudis, M. Tsanakopoulou, *J. Org. Chem.* **2003**, 68, 5627–5631.
- [10] K. Spagou, E. Malamidou-Xenikaki, S. Spyroudis, *Molecules* **2005**, 10, 226–237.
- [11] S. Koulouri, E. Malamidou-Xenikaki, S. Spyroudis, M. Tsanakopoulou, *J. Org. Chem.* **2005**, 70, 8780–8784.
- [12] E. Malamidou-Xenikaki, S. Spyroudis, M. Tsanakopoulou, H. Krautscheid, *J. Org. Chem.* **2007**, 72, 502–508.
- [13] a) P. Fuentealba, H. Preuss, H. Stoll, L. V. Szentpaly, *Chem. Phys. Lett.* **1982**, 89, 418–422; b) A. Bergner, M. Dolg, W. Kuechle, H. Stoll, H. Preuss, *Mol. Phys.* **1993**, 80, 1431–1441; c) P. Fuentealba, L. V. Szentpaly, H. Preuss, H. Stoll, *J. Phys. B* **1985**, 18, 1287–1296; d) G. Igel-Mann, H. Stoll, H. Preuss, *Mol. Phys.* **1988**, 65, 1321–1328; e) M. Dolg, U. Wedig, H. Stoll, H. Preuss, *J. Chem. Phys.* **1987**, 86, 866–872; f) M. Dolg, H. Stoll, H. Preuss, R. M. Pitzer, *J. Phys. Chem.* **1993**, 97, 5852–5859.
- [14] M. J. Frisch, G. W. Trucks, H. B. Schlegel, G. E. Scuseria, M. A. Robb, J. R. Cheeseman, J. A. Montgomery Jr., T. Vreven, K. N. Kudin, J. C. Burant, J. M. Millam, S. S. Iyengar, J. Tomasi, V. Barone, B. Mennucci, M. Cossi, G. Scalmani, N. Rega, G. A. Petersson, H. Nakatsuji, M. Hada, M. Ehara, K. Toyota, R. Fukuda, J. Hasegawa, M. Ishida, T. Nakajima, Y. Honda, O. Kitao, H. Nakai, M. Klene, X. Li, J. E. Knox, H. P. Hratchian, J. B. Cross, C. Adamo, J. Jaramillo, R. Gomperts, R. E. Stratmann, O. Yazyev, A. J. Austin, R. Cammi, C. Pomelli, J. W. Ochterski, P. Y. Ayala, K. Morokuma, G. A. Voth, P. Salvador, J. J. Dannenberg, V. G. Zakrzewski, S. Dapprich, A. D. Daniels, M. C. Strain, O. Farkas, D. K. Malick, A. D. Rabuck, K. Raghavachari, J. B. Foresman, J. V. Ortiz, Q. Cui, A. G. Baboul, S. Clifford, J. Cioslowski, B. B. Stefanov, G. Liu, A. Liashenko, P. Piskorz, I. Komaromi, R. L. Martin, D. J. Fox, T. Keith, M. A. Al-Laham, C. Y. Peng, A. Nanayakkara, M. Challacombe, P. M. W. Gill, B. Johnson, W. Chen, M. W. Wong, C. Gonzalez, J. A. Pople, *Gaussian 03*, Revision B.03, Gaussian, Inc., Pittsburgh, PA, **2003**.
- [15] a) S. H. Vosko, L. Wilk, M. Nusair, *Can. J. Phys.* **1980**, 58, 1200–1211; b) J. Baker, M. Muir, J. Andzelm, A. Scheiner in *ACS Symposium Series 629: Chemical Applications of Density-Functional Theory* (Eds.: B. B. Laird, R. B. Ross, T. Ziegler), American Chemical Society, Washington, DC, **1996**; c) L. A. Curtiss, K. Raghavachari, P. C. Redfern, J. A. Pople, *J. Chem. Phys.* **1997**, 106, 1063–1079.
- [16] M. P. Head-Gordon, M. J. Frisch, *Chem. Phys. Lett.* **1988**, 153, 503–506.
- [17] a) C. Gonzalez, H. B. Schlegel, *J. Chem. Phys.* **1989**, 90, 2154–2161; b) C. Gonzalez, H. B. Schlegel, *J. Phys. Chem.* **1990**, 94, 5523–5527.
- [18] E. D. Glendening, J. K. Badenhoop, A. E. Reed, J. E. Carpenter, J. A. Bohmann, C. M. Morales, F. Weinhold, *NBO 5.0*, Theoretical Chemistry Institute, University of Wisconsin, Madison, **2001**.
- [19] a) S. Dapprich, G. Frenking, *J. Phys. Chem.* **1995**, 99, 9352–9362; b) G. Frenking, N. Frohlich, *Chem. Rev.* **2000**, 100, 717–774.
- [20] S. I. Gorelsky, A. B. P. Lever, *J. Organomet. Chem.* **2001**, 635, 187–196.

Received: November 16, 2007

Published Online: February 13, 2008